Development 134, 4405-4415 (2007) doi:10.1242/dev.009118

Cross-regulation of *Ngn1* and *Math1* coordinates the production of neurons and sensory hair cells during inner ear development

Steven Raft[1], Edmund J. Koundakjian[2], Herson Quinones[3], Chathurani S. Jayasena[1], Lisa V. Goodrich[2], Jane E. Johnson[3], Neil Segil[1,4,*] and Andrew K. Groves[1,4,*]

Temporal and spatial coordination of multiple cell fate decisions is essential for proper organogenesis. Here, we define gene interactions that transform the neurogenic epithelium of the developing inner ear into specialized mechanosensory receptors. By Cre-loxP fate mapping, we show that vestibular sensory hair cells derive from a previously neurogenic region of the inner ear. The related bHLH genes *Ngn1* (*Neurog1*) and *Math1* (*Atoh1*) are required, respectively, for neural and sensory epithelial development in this system. Our analysis of mouse mutants indicates that a mutual antagonism between *Ngn1* and *Math1* regulates the transition from neurogenesis to sensory cell production during ear development. Furthermore, we provide evidence that the transition to sensory cell production involves distinct autoregulatory behaviors of *Ngn1* (negative) and *Math1* (positive). We propose that *Ngn1*, as well as promoting neurogenesis, maintains an uncommitted progenitor cell population through Notch-mediated lateral inhibition, and *Math1* irreversibly commits these progenitors to a hair-cell fate.

KEY WORDS: Proneural gene, bHLH, Hair cells, Inner ear, Otocyst, Neurogenesis

INTRODUCTION

During ear development, diverse components of a sensory pathway – neurons, mechanosensory hair cells, supporting cells and other non-sensory epithelial cells – derive from a simple ectodermal placode. These cell fate decisions are temporally and spatially regulated over a period when the placode, through growth and morphogenesis, transforms into an otocyst and, later, the inner ear labyrinth (see Fig. 1A) (Barald and Kelly, 2004; Kiernan et al., 2002). Early on, a subset of otic epithelial cells expresses neural fate markers (Raft et al., 2004; Cole et al., 2000; Adam et al., 1998), delaminates from the otocyst, and forms the VIIIth cranial ganglion rudiment with neural crest-derived glial precursors (D'Amico-Martel and Noden, 1983). In mice, hair cell production begins about 3.5 days after the onset of neurogenic gene expression (Shailam et al., 1999). Hair cells and supporting cells remain epithelial and form six discrete sensory patches along the inner ear labyrinth (Sher, 1971). Five sensory epithelia mediate the sense of balance (the utricular macula, saccular macula, and three cristae) and one – the organ of Corti – detects sound.

Morphological and genetic homologies between the sensory organs of the vertebrate ear and insects raise the question of whether neurons and hair cells derive from a common progenitor cell type (Fekete and Wu, 2002; Adam et al., 1998). Direct evidence for this is limited to one recent study in chicken that found clonal relatives of VIIIth ganglion neurons within the utricular macula and adjacent non-sensory epithelium (Satoh and Fekete, 2005). Existing evidence for such a relationship in mammals is circumstantial (Matei et al., 2005; Raft et al., 2004).

[1]Gonda Department of Cell and Molecular Biology, House Ear Institute, 2100 West 3rd Street, Los Angeles CA 90057, USA. [2]Department of Neurobiology, Harvard Medical School, 220 Longwood Avenue, Boston, MA 02115, USA. [3]Center for Basic Neuroscience, UT Southwestern Medical Center, Dallas, TX 75390, USA. [4]Department of Cell and Neurobiology, Keck School of Medicine, University of Southern California, Los Angeles, CA 90033, USA.

*Authors for correspondence (e-mails: nsegil@hei.org; agroves@hei.org)

Accepted 19 September 2007

Otic neurogenesis and hair cell generation are each dependent on an Atonal-related bHLH transcription factor. neurogenin 1 (*Ngn1*; also known as *Neurog1* – Mouse Genome Informatics) is necessary for the commitment of otocyst epithelial cells to a neural fate, as $Ngn1^{-/-}$ embryos lack an VIIIth cranial ganglion and fail to express neural fate markers in the otocyst (Ma et al., 1998; Ma et al., 2000). By contrast, *Math1* (also known as *Atoh1* – Mouse Genome Informatics) is necessary and sufficient for hair cell generation (Bermingham et al., 1999; Zheng and Gao, 2000; Izumikawa et al., 2005). Thus, during ear development, *Ngn1* and *Math1* function as determination factors, but it is not known whether their expression is regulated in a coordinated manner. In other neural systems, bHLH genes cross-regulate to control the commitment of progenitor cells to alternative fates (Bertrand et al., 2002). Examples include the involvement of Mash/Math/*Ngn1* genes in the sequential production of retinal neurons and glia (Inoue et al., 2002; Akagi et al., 2004), and in the simultaneous production of distinct neural subtypes in the forebrain and spinal cord (Fode et al., 2000; Gowan et al., 2001).

Here, we identify a progenitor cell field that produces both neurons and hair cells and describe genetic interactions mediating a neural-hair cell fate decision. We show that neural precursor and hair cell production overlap in the otic epithelium for several days and demonstrate by fate mapping that the *Ngn1*-expressing neurogenic region is transformed into the sensory maculae of the utricle and saccule. We propose that this transformation is governed by a mutual antagonism between *Ngn1* and *Math1*. We also show that *Ngn1* negatively regulates its own expression through Notch-mediated lateral inhibition, whereas *Math1* positively regulates its own expression. Differential autoregulation of *Ngn1* and *Math1* provides an explanation for the progression toward sensory epithelial development over time. *Ngn1*, as well as generating neural precursors, functions via lateral inhibition to maintain an uncommitted progenitor cell population for sensory epithelial development; *Math1*, in turn, irreversibly commits these progenitors to a hair cell fate.

MATERIALS AND METHODS

Experimental animals

Targeted disruptions of *Math1* (Ben-Arie et al., 1997), *Ngn1* (Ma et al., 1998), or *Pofut1* (Shi and Stanley, 2003) loci were maintained on a CD1 background. Ngn1-GFP and Ngn1-CreER BAC transgenic mice were constructed with RPCI-23-457E22 (http://bacpac.CHORI.org/), which contains a genomic insert of 184 kb with 113 kb 5′ and 71 kb 3′ of the *Ngn1* coding sequence. The Math1-GFP BAC transgenic was constructed with RPCI-23318G16, which contains a genomic insert of 181 kb with 75 kb 5′ and 104 kb 3′ of the *Math1* coding sequence. Homologous recombination in bacteria (Yang et al., 1997) was used to replace endogenous coding sequences with coding sequence for either nuclear-localized EGFP (Clontech) or CreER^{T2} (Feil et al., 1997). Details of Ngn1CreER BAC transgene construction (E.J.K. and L.V.G., unpublished) are available on request. Genotyping was accomplished by PCR using the following oligos: Ngn1-GFP, 5′-CGAAGGCTACGTCCAGGAG-CGCAC-3′ and 5′-GCACGGGGCCGTCGCCGATGGGGGTGT-3′; Ngn1-CreER, 5′-AGCCCATTCACTCCCTGAG-3′ and 5′-ATCAACGTTTTCT-TTTCGGA-3′; Math1-GFP, 5′-CTGACCCTGAAGTTCATCTGCACC-3′ and 5′-TGGCTGTTGTAGTTGTACTCCAGC-3′; Math1 mutants, 5′-GAA-CCCAAAGACCTTTTGCAC-3′ and 5′-CACGAGACTAGTGAGACGTG-3′; Ngn1 mutants, 5′-AAGAGTGCCATGCCCGAAGG-3′ and 5′-AAGG-CCGACCTCCAAACCTC-3′; Pofut1 mutants, 5′-GGGTCACCTTCAT-GTACAAGTGAGTG-3′ and 5′-ACCCACAGGCTGTGCAGTCTTTG-3′. The Math1-GFP transgenic line carrying a 1.4 kb *Math1* enhancer fragment was genotyped as previously described (Chen et al., 2002; Lumpkin et al., 2003). The Ngn1-CreER transgene was maintained in males on a Z/EG reporter strain (Novak et al., 2000); double-transgenic embryos were obtained by breeding these to Z/EG reporter females. Tamoxifen (Sigma T5648) in corn oil was administered by gavage twice daily to alert, pregnant females (1.0 mg per 40 g of body weight per administration).

Immunohistochemistry and in situ hybridization

Embryos were immersion-fixed (4% paraformaldehyde), cryoprotected in 30% sucrose in PBS, embedded in OCT compound (Tissue-Tek) and cryosectioned. Immunohistochemistry was performed by a standard protocol of blocking (5% donkey serum, 0.1% Triton X-100 in PBS), incubations and washings. Antibodies included: anti-myosin VIIa rabbit polyclonal (obtained from Tama Hasson, UCSD, CA; 1:400), anti-GFP chicken polyclonal (Chemicon, 1:100), anti-GFP rabbit polyclonal (Molecular Probes, 1:1000), anti-islet1/2 mouse monoclonal (mAb4D5, Developmental Studies Hybridoma Bank, straight supernatant) and anti-human/mouse active caspase 3 (R&D Systems, 1:500). Secondary antibodies (Jackson ImmunoResearch)

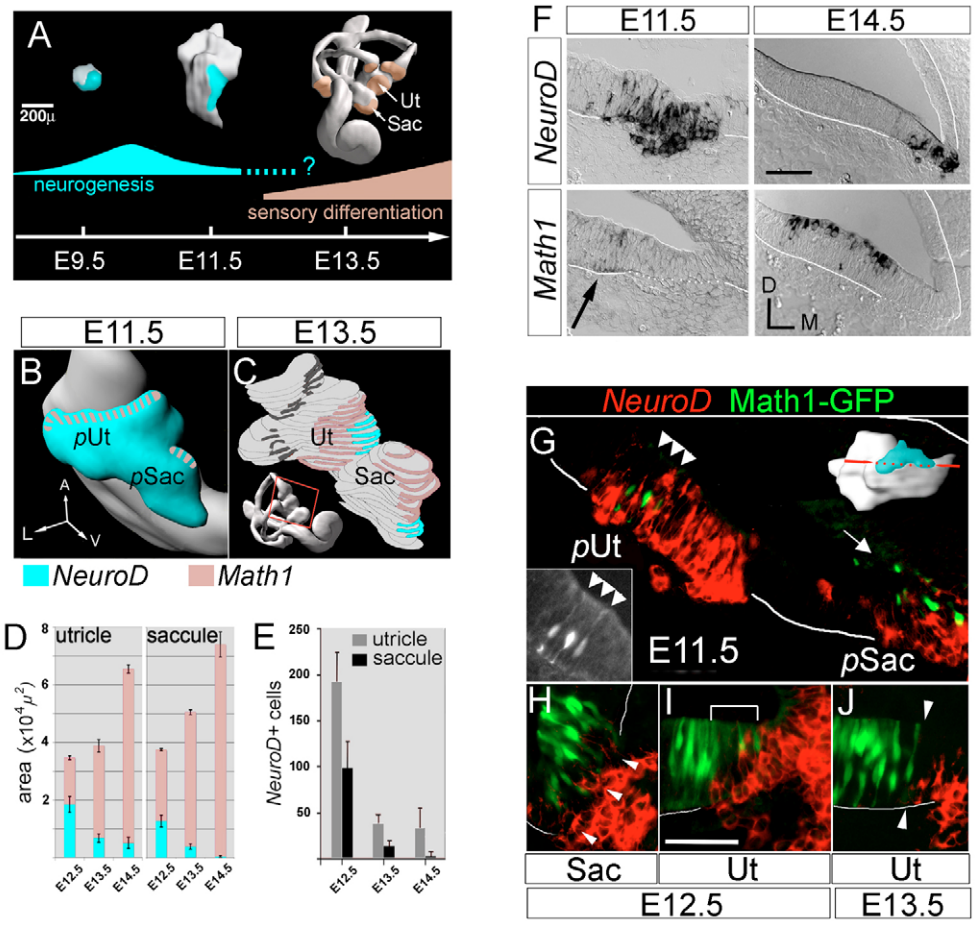

Fig. 1. Neurogenesis and hair cell production coincide in the otic epithelium. (**A**) Temporal-spatial relationships between neurogenesis (cyan) and sensory epithelial differentiation (beige). Activity levels are schematized in color above the time-line. Ut, utricle; Sac, saccule. (**B**) E11.5 otocyst (rotated from A) with *NeuroD* domain (cyan) and *Math1* expression (beige hatching) highlighted. *p*Ut, presumptive utricle; *p*Sac, presumptive saccule. (**C**) Part of the early inner ear labyrinth at E13.5, defined by the red box, shown on same scale as B. Orientation and color codes are as in B. *Math1* expression in the anterior and lateral cristae is shown in dark gray. (**D**) *NeuroD* (cyan) and *Math1* (beige) epithelial expression domain areas versus developmental stage. (**E**) Epithelial *NeuroD*$^+$ cell number versus developmental stage. (**F**) Alternating serial sections through the presumptive (E11.5) and definitive (E14.5) utricle, hybridized for *NeuroD* or *Math1*. Arrow indicates early *Math1* expression. (**G-J**) Math1-GFP reporter tissue double-labeled with *NeuroD* antisense RNA (red) and anti-GFP antibody (green). In G, triple arrowheads and arrow indicate lateral and medial stripes of Math1-GFP, respectively, as illustrated in B. In H and I, arrowheads and bracket indicate spatial overlap of the two markers. Arrowheads in J indicate the border of Math1-GFP and *NeuroD* expression. Axes in F apply to F-J. Scale bars: 50 μm.

were used at 1:200. In situ hybridization was performed by standard methods (Stern, 1998). For combined in situ hybridization and GFP immunohistochemistry (with anti-GFP rabbit polyclonal, Molecular Probes), proteinase K digestion (5 μg/ml in PBS) was reduced to 3 minutes. Digoxygenin-labeled RNA probes for *NeuroD* (Lee et al., 1994), *Math1* (Helms and Johnson, 1998), *Ngn1* (Ma et al., 1998) and *Dll1* (Beckers et al., 1999) were prepared by standard methods. TUNEL reactions were performed according to manufacturer's instructions (Roche).

Quantitative analyses and three-dimensional reconstructions

Serial sections were photographed and imported into Photoshop CS2 (Adobe). Occurrence data were obtained by digitally marking all positive cells identified in TIFF files of complete, consecutive 12 μm serial sections for a given structure and automated tallying (Image Processing Toolkit, Reindeer Graphics). Data were tested for significance with multiple *t*-tests (two-tailed; unequal variance). Domain areas and relative cell positions were quantified with NIHimage/ImageJ. Space filling models were generated by aligning serial sections with Autoaligner (Bitplane AG), tracing the regions of interest, and importing stacks of tracings into Imaris (Bitplane AG).

RESULTS

Neurogenesis and hair cell production overlap spatially and temporally in the developing utricle and saccule

We performed RNA in situ hybridization for *NeuroD* and *Math1* to characterize any temporal and spatial overlap between neurogenesis and hair cell production (Fig. 1A) (Fritzsch et al., 2002). *NeuroD* (also known as *Neurod1* – Mouse Genome Informatics), a neural differentiation gene (Bertrand et al., 2002), is expressed under the control of *Ngn1* in the otic epithelium (Ma et al., 1998) and marks cells that are committed to the neural lineage. We also hybridized a *NeuroD* RNA probe to tissue from a Math1-GFP transgenic reporter mouse (Lumpkin et al., 2003). *Math1* is the earliest known specific marker of hair cells (Bermingham et al., 1999).

The number of *NeuroD*$^+$ cells within the epithelium increases between E9 and E10.5 (Raft et al., 2004) (Fig. 1A). Between E11.5 and E12.5, *NeuroD* expression split into two distinct regions of neurogenesis that would ultimately lie within the developing utricle and saccule (Fig. 1B,C, cyan). Neurogenesis declined from E11.5 onward (Fig. 1D,E), but a few delaminating *NeuroD*$^+$ cells were still present in the utricle as late as E17.5 (5±4 cells, *n*=3 ears; data not shown). A comparison of *NeuroD* and *Ngn1* expression in the otic epithelium revealed no differences in their patterning (see Fig. S1A,D,E,H in the supplementary material).

During the decline in neurogenesis, *Math1* mRNA expression begins and is maintained in all hair cells through to at least E17.5 (Shailam et al., 1999). At E11.5, two *Math1*$^+$ stripes appeared within the *NeuroD* domain along its lateral and medial borders (Fig. 1B,F,G). Between E11.5 and E12.5, Math1-GFP$^+$ cells in these stripes increased in number by 8- to 10-fold and formed the nascent maculae of the utricle and saccule. Initially, Math1-GFP$^+$ and *NeuroD*$^+$ cells intermingled (Fig. 1H,I), but later lay on either side of a border that delineates the macula and its adjacent neurogenic domain (Fig. 1J). *Math1* expression associated with the cristae first appeared as separate foci outside the *NeuroD*$^+$ domain at around E12 (data not shown). We found no temporal overlap of *Math1* and *NeuroD* expression in the cochlea (data not shown), suggesting that neurogenesis and hair cell generation do not coincide in the auditory end-organ. Taken together, our data reveal that neurogenesis is maintained through stages of hair cell production in the utricle and saccule, but declines sharply as *Math1* expression and hair cell production increase.

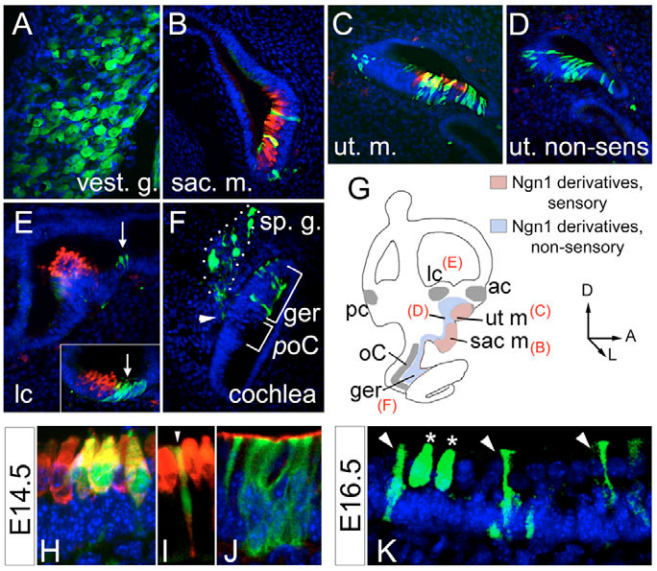

Fig. 2. Fate mapping identifies Ngn1 derivatives in the VIIIth ganglion and ear epithelium. (**A-F**) Structures from E16.5 (A) or E14.5 (B-F) Ngn1-CreER;Z/EG embryos, double-stained for transgenic GFP (green, Ngn1 derivatives) and myosin VIIa (red, sensory hair cells). ac, anterior crista; ger, greater epithelial ridge; lc, lateral crista; oC, organ of Corti, pc, posterior crista; poC, presumptive organ of Corti; sac. m., saccular macula; sp. g. spiral ganglion; ut. m. utricular macula; ut. non-sens, utricular non-sensory; vest. g., vestibular ganglion. Arrows in E and inset indicate Ngn1 derivatives in non-sensory tissue between the lateral crista and utricular macula. (**G**) Summary of Ngn1 derivatives in the ear. Gray areas represent sensory structures lacking Ngn1 derivatives. (**H-K**) Ngn1 derivative cell phenotypes (green) in sensory maculae. Red label is myosin VIIa in H,I and phalloidin in J. Arrowhead in I indicates a double-positive cell. In K, arrowheads indicate supporting cells; asterisks indicate hair cells.

Maculae of the utricle and saccule derive from the *Ngn1*-expressing domain of the otocyst

Our expression analysis raised the possibility that sensory maculae of the utricle and saccule, but not the cristae or organ of Corti, derive from the neurogenic region of the otocyst. To test this, we permanently labeled cells of the neurogenic region using a BAC transgenic mouse line (Ngn1-CreER) (E.J.K. and L.V.G., unpublished) that expresses a tamoxifen-inducible form of Cre recombinase (CreER) under the control of *Ngn1* regulatory elements (see Fig. S1B,F in the supplementary material). This allowed us to identify cells transiently expressing *Ngn1* and their progeny after sensory epithelia have formed. As expected, when the Ngn-CreER mouse was crossed with the Z/EG reporter line (Novak et al., 2000) and tamoxifen administered, roughly 50% of VIIIth cranial ganglion neurons were permanently labeled in double-transgenic embryos (Fig. 2A; see Fig. S1I in the supplementary material). Importantly, we also found Ngn1 derivatives to be present in sensory and non-sensory inner ear epithelia of embryos that had been sacrificed after neurogenesis was largely complete (Fig. 2B-G).

To follow the fate of *Ngn1*-expressing cells in the ear, we administered tamoxifen twice daily from E8.5 until E13.5 to pregnant females of Ngn1-CreER × Z/EG matings. We analyzed 20 double-transgenic right ears from seven litters ranging in age from E13.5-16.5 and identified over 5000 labeled epithelial cells. Sensory epithelia were identified by the presence of myosin VIIa protein, and the resulting distribution pattern of epithelial Ngn1 derivatives is

summarized in Fig. 2G. Supporting the hypothesis that maculae are the only sensory epithelia to derive from neurogenic epithelium, Ngn1 derivatives were present in the utricular and saccular maculae of all specimens analyzed (Fig. 2B,C). For embryos sacrificed at E14.5, tamoxifen administration from E8.5-13.5 yielded an average of 157±25 Ngn1 derivatives per utricular macula (n=6 ears from two litters). We found a lower occurrence of such cells in the saccular macula (82±24; n=6 ears from two litters). By contrast, only one ear out of the 20 analyzed had Ngn1 derivatives in the lateral crista (eight labeled supporting cells), and no such cells were detected in the other cristae in our cohort of specimens. No Ngn1 derivatives were detected in the organ of Corti. We were able to classify macular Ngn1 derivatives as differentiated myosin VIIa$^+$ hair cells (Fig. 2H), undifferentiated myosin VIIa$^+$ epithelial cells migrating within the apical-basal plane of the epithelium (Fig. 2I), or as myosin VIIa$^-$ pseudostratified epithelial cells (Fig. 2J). By E16.5, many of these myosin VIIa$^-$ Ngn1 derivatives exhibited morphological features of supporting cells (Fig. 2K, arrowheads).

Regions of non-sensory epithelium flanking the maculae of E13.5-16.5 ears also contain labeled cells (Fig. 2D,E), but we found no Ngn1 derivatives in the semicircular canals. In the auditory portion of the ear, Ngn1 derivatives were detected in 82% (14/17) of the cochleae analyzed (E13-16.5), but showed extreme variability in their numbers (93±146 cells, n=8 cochleae at E14.5). These cells commonly occupied the greater epithelial ridge (GER), a non-sensory region of the cochlea that is adjacent to the organ of Corti (Fig. 2F). However, as described above, no Ngn1 derivatives were detected in the organ of Corti itself.

Administration of tamoxifen only at placode/otocyst stages (E8.5 and E9.5) resulted in the same spatial distribution of Ngn1 derivatives as described above. Together, our results indicate that the utricular and saccular maculae, as well as some non-sensory epithelium flanking these structures, derive from the neurogenic region of the otocyst, and that *Ngn1*-expressing otocyst cells or their descendants can differentiate as hair cells, supporting cells, or as structural epithelial cells.

The *Ngn1* domain contracts gradually and stereotypically in the primordia of the utricle and saccule

To understand how the sensory maculae and their surrounding tissue arise from neurogenic tissue, we analyzed changes in *Ngn1* expression over time using two different transgenic lines. A series of Ngn1-CreER × Z/EG litters received initial tamoxifen exposures at progressively later developmental time points from E8.5 onwards; once begun, tamoxifen administration was continued twice per day until E13.5 and all litters were sacrificed on E14.5. By quantifying GFP$^+$ cells in the utricle of these embryos, we confirmed that starting tamoxifen administration at progressively later times leads to diminishing numbers of labeled Ngn1 derivatives (Fig. 3C). From these experiments, we mapped the distributions of Ngn1 derivatives in the utricular macula and its flanking non-sensory tissue (Fig. 3E-E‴). The distribution of cells actively expressing *Ngn1* at E14.5 was obtained from a different BAC transgenic line (Ngn1-GFP) that reports directly on *Ngn1* promoter activity (see Fig. S1C,G,J in the supplementary material).

Our results for the utricle are consistent with a stereotyped reduction in the area of *Ngn1* expression over time. At E14.5, the active neurogenic domain of the utricle, defined by expression of the Ngn1-GFP reporter, lay medial to and centered along the anteroposterior axis of the macula (Fig. 3A,B). When tamoxifen was administered to Ngn1-CreER;Z/EG litters from E8.5-13.5 (Fig. 3E), Ngn1 derivatives were present throughout the neurogenic domain (white region), the macular sensory epithelium (gray region, defined by myosin VIIa expression), lateral non-sensory tissue (between the utriclar macula and lateral crista, yellow region), and posterior non-sensory tissue (between the utricular and saccular maculae, yellow region, bottom). When tamoxifen was administered from E10.5 or E11.5 to E13.5, Ngn1 derivatives were present at all these sites, except for posterior non-sensory tissue (between the maculae, Fig. 3E′). Finally, when tamoxifen was administered from E12.5-13.5, Ngn1 derivatives were present only within the neurogenic domain and a portion of the macular epithelium nearest its border with the neurogenic domain (Fig. 3E″). Contraction of the *Ngn1* expression domain is therefore directional, occurring largely from lateral to medial in the utricle. We observed similar *Ngn1* expression dynamics in the saccule (see Fig. S2 in the supplementary material), although contraction occurred largely along the anteroposterior axis of this structure, rather than along the medial-lateral axis as in the utricle. Importantly, all tamoxifen start times tested (ranging from E8.5-12.5) resulted in a cohort of macular Ngn1 derivatives comprising both hair cells and pseudostratified epithelial cells. These data, together with results described in the previous section, indicate that macular sensory cells can derive from cells that express *Ngn1* at any time between E9 and E14.

Math1 suppresses neurogenesis in the developing utricle and saccule

Our results indicate that the domain of *Ngn1*$^+$ precursor cells is gradually transformed from a purely neurogenic region into sensory epithelia of the utricular and saccular maculae. Since functional antagonism between related bHLH transcription factors has been described in other systems (Fode et al., 2000; Gowan et al., 2001; Akagi et al., 2004), we tested whether Math1 (which is required for sensory epithelial differentiation) (Bermingham et al., 1999) suppresses neurogenesis by inhibiting *Ngn1* transcription in otic epithelial cells. We found that *Math1* function is required for the normal contraction of epithelial *Ngn1* expression characterized in the previous section (Fig. 4A,B; data not shown). We quantified expression of the Ngn1-GFP reporter and *NeuroD* in *Math1*-null homozygote embryos and observed large (>6×) increases over wild type in the numbers of neural precursors within the developing utricle and saccule; a less severe form of this phenotype was found in *Math1* heterozygotes (Table 1). Excess neural precursors were seen to delaminate and migrate away from the mutant epithelium to form an VIIIth cranial ganglion that was larger than wild type (see Fig. S3B asterisk, E-H, in the supplementary material). Ectopic neurogenesis in *Math1*$^{-/-}$ epithelia localized specifically to parts of the utricle and saccule that normally differentiate as sensory maculae, and was not detected in the cristae, cochlea, or any non-sensory epithelia (Fig. 4D,F; see Fig. S3A-D in the supplementary material; data not shown); in *Math1* heterozygotes, it occurred only at the interface of neurogenic and sensory regions (Fig. 4E, bracket). In *Math1*$^{-/-}$ epithelia, marked excess neurogenesis at E14.5 and E15.5 followed a partial decline in neurogenic activity through E13.5 (Fig. 4N). This initial declining trend in neurogenic activity in mutants, which is similar to that of wild type, suggests that factors in addition to *Math1* contribute to early neurogenic suppression.

Reduced *Ngn1* gene dose causes excess and ectopic *Math1* expression in the developing utricle and saccule

Ngn1 loss-of-function causes a failure of neural precursor generation in the otic epithelium and absence of the VIIIth cranial ganglion (Ma et al., 1998; Ma et al., 2000). If antagonism between *Math1* and

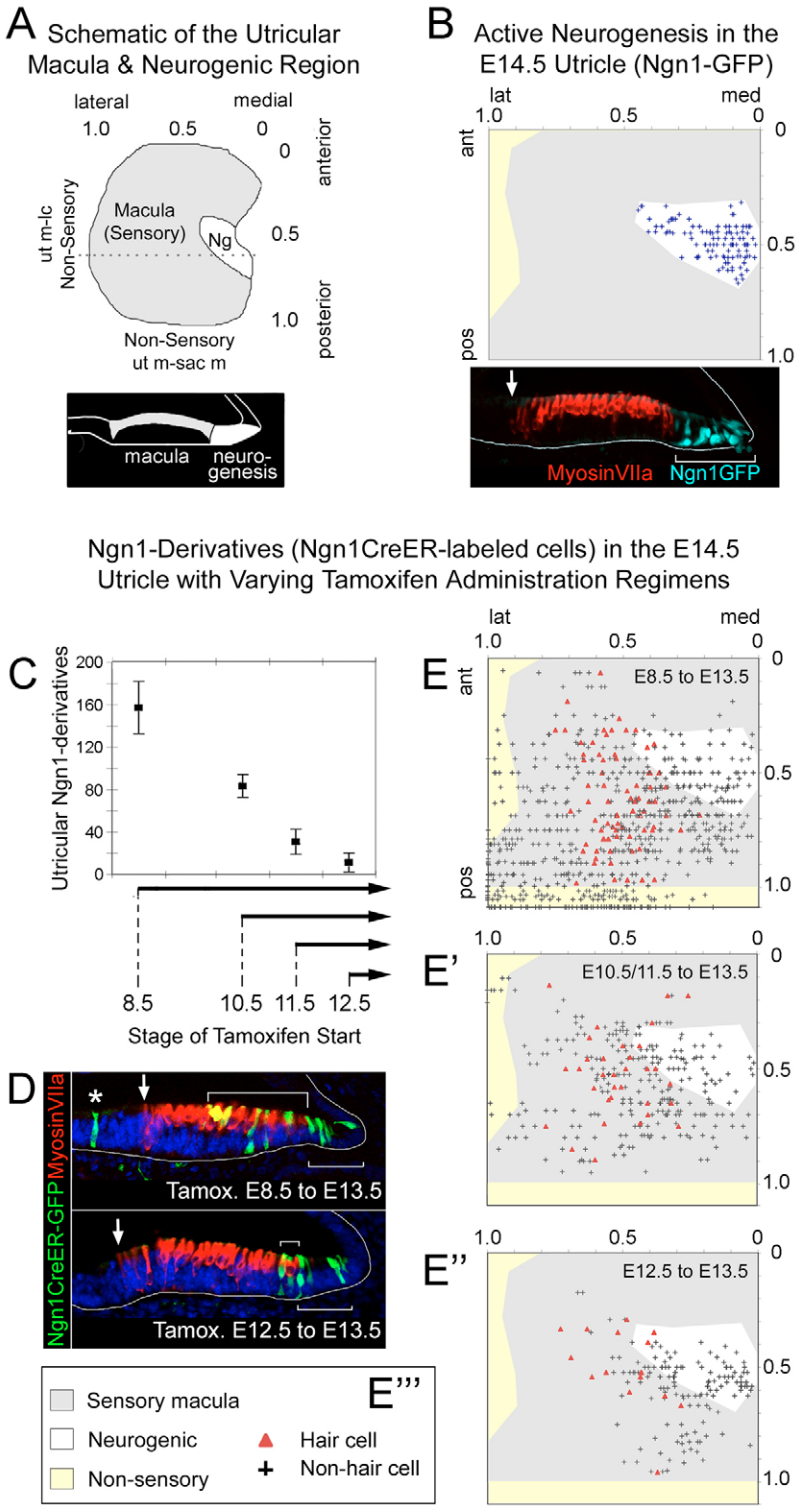

Fig. 3. *Ngn1* expression decreases over time in the prospective utricle. (**A**) E14.5 utricular macula schematized in the same orientation as the scatterplots in B and E-E″. A cross-section of the macula along the dotted line is represented at the bottom. The macula (region of myosin VIIa staining) is in gray. The active neurogenic region (Ng, region of Ngn1-GFP staining) is white. ut m-lc, non-sensory tissue between the utricular macula and lateral crista; ut m-sac m, non-sensory tissue between the utricular macula and saccular macula. (**B**) Distribution of GFP$^+$ cells (blue crosses, cyan in image) from three E14.5 Ngn1-GFP BAC transgenic utricles, plotted on a normalized scale, defines the region of active neurogenesis. Gray area represents an averaged macular area (myosin VIIa $^+$); the yellow area is non-sensory epithelium between the utricular macula and lateral crista. White arrow marks the lateral extent of the macula. (**C**) Number of Ngn1 derivatives in the Ngn1-CreER;Z/EG utricle versus time of first tamoxifen feeding for embryos sacrificed at E14.5. Each point is based on four or more ears from two or more litters. (**D**) Sections through utricular maculae, representing the change in the spatial distribution of Ngn1 derivatives (green) with different tamoxifen regimens. Downturned brackets indicate overlap between Ngn1 derivatives and myosin VIIa $^+$ hair cells. Upturned brackets indicate the region of active neurogenesis. White arrows indicate the lateral extent of the macula. Asterisk shows an Ngn1 derivative in non-sensory tissue between the utricular macula and lateral crista. (**E-E‴**) Spatial distributions of Ngn1 derivatives from E14.5 utricles exposed to different tamoxifen administration regimens, as indicated at the top of each plot. (E) *n*=4 utricles; (E′) *n*=6 utricles; (E″) *n*=14 utricles. Ngn1 derivative cell types and regions of the plot are coded as shown in E‴.

Ngn1 during ear development is reciprocal, then *Ngn1* loss-of-function should result in ectopic hair cells. Our analysis of sensory marker expression in the *Ngn1*$^{-/-}$ utricle confirmed this prediction. As indicated by both *Math1* and myosin VIIa expression, the *Ngn1*$^{-/-}$ utricular macula at E13.5 and E14.5 was expanded medially into the region that is normally neurogenic (Fig. 4C,F,H,K,M). At E13.5, the total area of *Math1* expression in the *Ngn1*$^{-/-}$ utricle exceeded that of wild type by 39% (P<0.002, n=3 epithelia per genotype), and there were more *Math1*$^+$ cells in the *Ngn1*$^{-/-}$ utricle than in wild type at E13.5 and E14.5 (Table 1). Growth abnormalities of the *Ngn1*$^{-/-}$ mutant ear (Matei et al., 2005; Ma et al., 2000) confounded our analysis of other structures. The saccule was profoundly hypoplastic (see Fig. S4A in the supplementary material), and we correlated this to a period of intense, region-specific apoptosis in the otic epithelium between E11.5 and E12.5 (see Fig. S4B,C in the supplementary material; data not shown).

Table 1. Occurrence of neural and sensory precursor cells in wild-type and mutant inner ear epithelia

	Marker	Stage	*Ngn1*$^{-/-}$	*Ngn1*$^{+/-}$	Wild type	*Math1*$^{+/-}$	*Math1*$^{-/-}$
Utricle	Ngn1-GFP	E14.5	0	89±16 [0.004 (5)]	50±16 [1.0 (11)]	76±12 [0.0003 (11)]	360±35 [0.003 (3)]
	NeuroD	E14.5	0	54±16 [0.04 (6)]	33±15 [1.0 (7)]	63±18 [0.04 (4)]	224±33 [0.006 (3)]
	Math1	E13.5	415±27 [0.02 (4)]	451±35 [0.0004 (7)]	361±35 [1.0 (7)]	n.d.	0
		E14.5	561±23 [0.0001 (6)]	623±55 [0.001 (6)]	484±17 [1.0 (5)]	n.d.	0
	myosin VIIa	E14.5	353±21 [0.00002 (4)]	377±37 [0.0005 (6)]	503±31 [1.0 (6)]	379±31 [0.0006 (4)]	0
Saccule	Ngn1-GFP	E14.5	0	25±6 [0.02 (3)]	1.3±0.8 [1.0 (6)]	13±4 [0.001 (5)]	190±54 [0.04 (3)]
	NeuroD	E14.5	0	6.7±2 [0.002 (6)]	2.3±1.9 [1.0 (7)]	6.8±0.5 [0.0007 (4)]	144±43 [0.03 (3)]
	Math1	E13.5	72±28 [0.0001 (4)]	440±37 [0.001 (7)]	354±39 [1.0 (7)]	n.d.	0
		E14.5	192±36 [<0.00001 (6)]	718±38 [0.001 (7)]	621±35 [1.0 (5)]	n.d.	0
	myosin VIIa	E14.5	71±30 [<0.00001 (4)]	387±102 [0.03 (4)]	584±23 [1.0 (4)]	433±40 [0.01 (3)]	0
Lateral crista	*Math1*	E14.5	340±31 [0.004 (6)]	448±55 [0.8 (8)]	454±51 [1.0 (5)]	n.d.	0

Values (mean±s.d.) for the occurrence of Ngn-GFP^{+}, *NeuroD*$^{+}$, *Math1*$^{+}$ and myosin VIIa^{+} cells within inner ear epithelia of wild-type and mutant embryos, with [*P*-value (number of ears sampled)]. *P*-values refer to two-tailed *t*-tests comparing mutant and wild type. Samples for each category were drawn from a minimum of three litters. n.d., Not determined.

Ngn1$^{-/-}$ cristae were also smaller than their wild-type counterparts, which was evident from our quantification of *Math1*$^{+}$ cells in the *Ngn1*-null mutant lateral crista (Table 1).

The inner ear of *Ngn1* heterozygotes was not grossly dysmorphic and therefore provided a context for analyzing cell fate changes in response to reduced *Ngn1* levels. We quantified *Math1*$^{+}$ cells in the utricle, saccule and lateral crista of *Ngn1* heterozygote and wild-type littermates. In the *Ngn1*$^{+/-}$ utricle and saccule, numbers of *Math1*$^{+}$ cells were increased by 16-29% compared with wild type (Table 1). This was due to an expansion in the area of *Math1*$^{+}$ macular domains in heterozygotes (Fig. 4K,L) and an increased density of *Math1*$^{+}$ cells within heterozygote maculae compared with wild type (Fig.

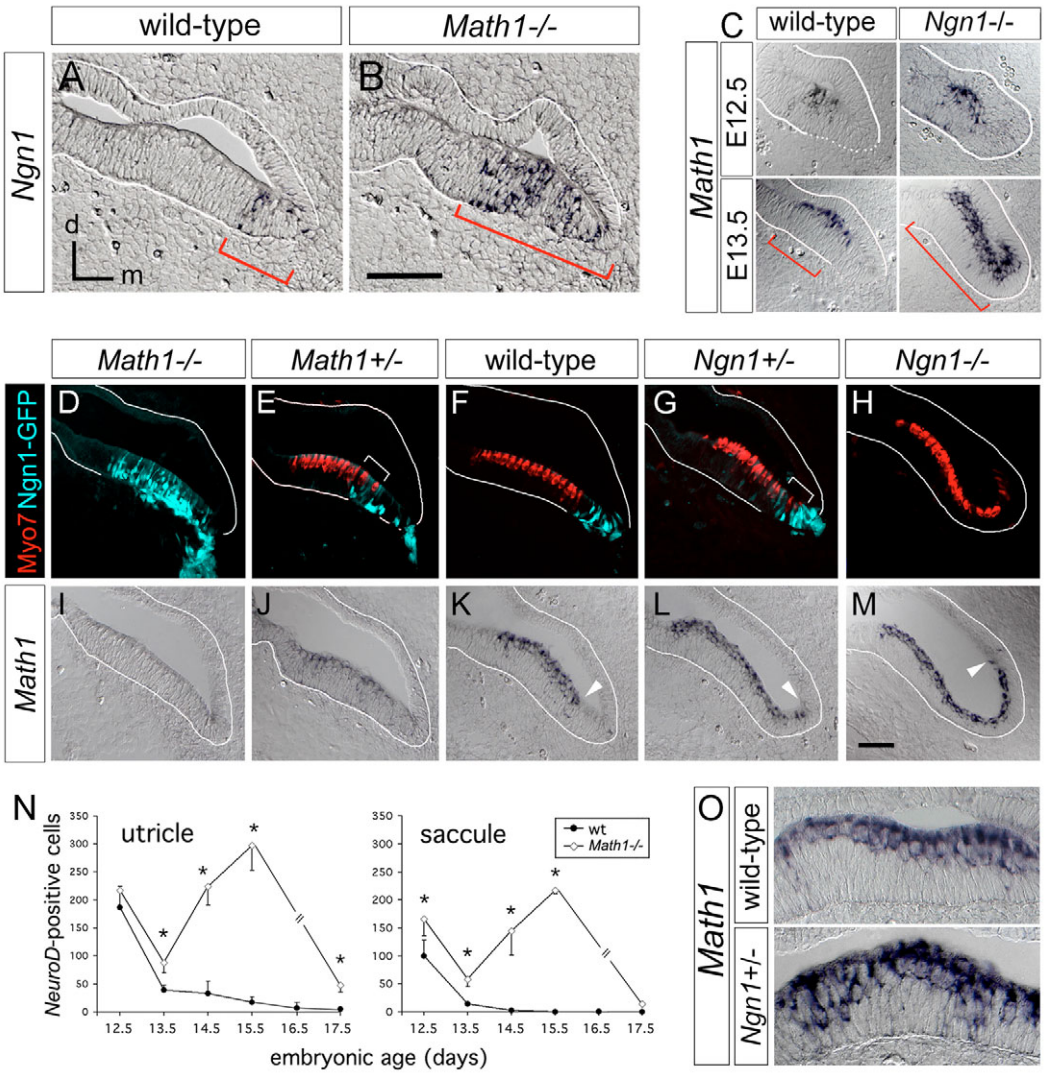

Fig. 4. Complementary phenotypes of *Math1* and *Ngn1* mutants. (**A**,**B**) Ectopic *Ngn1* expression in the E13.5 wild-type and *Math1*$^{-/-}$ utricle. Axes apply to all images. (**C**) Ectopic *Math1* expression in the E13.5 wild-type and *Ngn1*$^{-/-}$ utricle. (**D-M**) Expression of Ngn1-GFP transgene (cyan), myosin VIIa protein (red) and *Math1* mRNA in wild-type, *Math1* and *Ngn1* mutant utricles at E14.5. Brackets in E,G indicate abnormal overlap of neural precursors and hair cells in heterozygotes. Arrowheads in K-M indicate macular expansion in *Ngn1* mutants. (**N**) *NeuroD*$^{+}$ epithelial cell numbers in utricle and saccule of *Math1*$^{-/-}$ and wild-type littermates over time. Asterisks denote significance at $P<0.05$. Points represent the mean and standard deviation of three ears from separate litters. (**O**) Utricular maculae of wild-type and *Ngn1*$^{+/-}$ littermates at E14.5, hybridized identically for *Math1*. Scale bars: 50 μm.

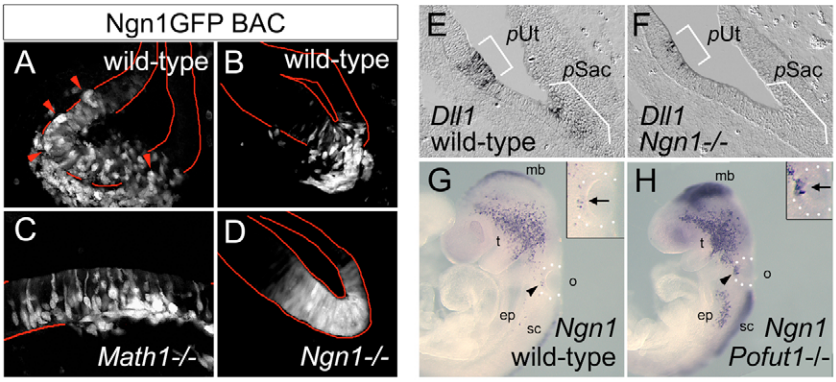

Fig. 5. *Ngn1* negatively autoregulates and interacts with the Notch pathway. (**A-D**) Ngn1-GFP BAC transgene expression in a wild-type E10 otocyst (A), wild-type E12.5 utricle (B), *Math1*$^{-/-}$ E14.5 utricle (C) and *Ngn1*$^{-/-}$ E12.5 utricle (D). Arrowheads in A indicate delaminating cells with stronger GFP signal than their neighbors. (**E**,**F**) *Dll1* expression in wild-type and *Ngn1*$^{-/-}$ otic epithelia at E11.5. *p*Ut, presumptive utricle; *p*Sac, presumptive saccule. (**G**,**H**) *Ngn1* mRNA expression in wild-type and *Pofut*$^{-/-}$ embryos at E9. Insets show the invaginating otic epithelium. Arrowheads and arrows (insets) indicate *Ngn1* mRNA signal in the otic epithelium, outlined with dotted white line. o, otic epithelium; mb, midbrain; t, trigeminal placode; ep, epibranchial placode; sp, spinal cord.

4O). Unlike the maculae, the *Ngn1*$^{+/-}$ lateral crista – a structure that does not express *Ngn1* during normal development – showed no increase in *Math1*$^{+}$ cells compared with wild type (Table 1). These results suggest that the numbers of *Math1*$^{+}$ cells are increased in response to *Ngn1* hemizygosity specifically at sites where the two genes are co-expressed (utricle and saccule).

Although, as described above, myosin VIIa expression domains are expanded in *Ngn1* mutants (Fig. 4F-H), we found fewer myosin VIIa^{+} cells in the *Ngn1*$^{-/-}$ utricle and *Ngn1*$^{+/-}$ utricle and saccule than in wild type (Table 1). This was owing to a lower density of myosin VIIa^{+} cells in the mutants as compared with wild type and, in addition, myosin VIIa^{+} hair cell size and shape were abnormal in the mutants (see Fig. S4D-F in the supplementary material). Neither TUNEL, nor anti-caspase 3 immunohistochemistry, at E14.5 provided evidence that these abnormalities were due to apoptosis (data not shown). Since the onset of myosin VIIa expression normally follows *Math1* expression, and all of the mutant sites under consideration have more *Math1*$^{+}$ cells than wild type, a considerable number of *Math1*$^{+}$ macular cells in *Ngn1* mutants (greater than 35%) must fail to express myosin VIIa^{+}. Taken together, our results indicate that at sites of *Ngn1* and *Math1* co-expression (utricle and saccule), reduced *Ngn1* gene dose causes excess numbers of *Math1*$^{+}$ cells to form, but many of these cells do not properly differentiate as hair cells.

Ngn1 negatively regulates its own expression and is inhibited by Notch signaling

Ngn1 is thought to function analogously to the *Drosophila* proneural genes (Ma et al., 1996; Ma et al., 1998; Cornell and Eisen, 2002). Consistent with a proneural function for *Ngn1*, we found that Ngn1-GFP signal varies in intensity between neighboring cells, and is strongest in delaminating cells (Fig. 5A). We therefore tested whether *Ngn1* negatively regulates its own transcription in the otic epithelium by comparing expression patterns of the Ngn1-GFP BAC transgene in *Ngn1*-null homozygote and wild-type littermates prior to the appearance of ectopic *Math1* expression. At E12.5, Ngn1-GFP is normally expressed in a speckled pattern by a subset of cells in the neurogenic region (Fig. 5B). By contrast, in *Ngn1*$^{-/-}$ embryos, the GFP signal was present in all cells of the region, with little variability in signal strength between cells (Fig. 5D). Loss of the speckled expression pattern for the Ngn1-GFP transgene did not occur on a *Math1*$^{-/-}$ background (Fig. 5C), indicating that this phenotype is specific to the loss of *Ngn1*. We also found excess Ngn1-GFP^{+} and *NeuroD*$^{+}$ epithelial cells in the *Ngn1*$^{+/-}$ utricle and saccule compared with wild type (Table 1). In *Ngn1*$^{-/-}$ ears, expression of the Ngn1-GFP transgene was completely abolished by E14.5, presumably owing to inhibition by ectopic *Math1* expression (Fig. 4H,M).

To investigate potential interactions of *Ngn1* with Notch signaling, we assayed expression of the Notch ligand *Dll1* in the *Ngn1*-null homozygote. We found reduced *Dll1* expression in the primitive utricle and saccule of mutants as compared with wild type (Fig. 5E,F) (see also Ma et al., 1998). To test whether Notch activity suppresses *Ngn1* transcription within the otic epithelium, we analyzed *Ngn1* expression in embryos lacking *Pofut1*. This gene encodes the protein O-fucosyltransferase 1, which glycosylates epidermal growth factor-like repeats within the extracellular domain of the Notch receptor (Lei et al., 2003; Okajima et al., 2003; Okajima et al., 2005). *Pofut1* loss-of-function abolishes ligand-induced Notch signaling and causes phenotypes similar to those of embryos lacking downstream effectors of all Notch receptors, including mid-embryonic lethality (Shi and Stanley, 2003). We therefore assayed *Ngn1* expression in early *Pofut1* embryos (E9-9.5), when the otic placode invaginates to first form an otocyst. At these stages, *Ngn1* mRNA signals were increased in *Pofut1*$^{-/-}$ embryos as compared with wild-type littermates in the otic epithelium, midbrain, trigeminal placode, epibranchial placodes and spinal cord (Fig. 5G,H), indicating that *Ngn1* transcription in all these embryonic regions is negatively regulated by canonical Notch signaling. Thus, the negative autoregulation of *Ngn1* in the otic epithelium might be controlled by Notch-mediated lateral inhibition.

Positive autoregulation of *Math1* in the inner ear epithelium

Math1 positively autoregulates its transcription at particular sites in the embryo (Helms et al., 2000). To determine whether *Math1* is subject to positive autoregulation during ear development, transgenic reporters of *Math1* promoter activity were compared across wild-type and *Math1*$^{-/-}$ backgrounds. A BAC that expresses GFP under the control of *Math1* regulatory elements mimics patterns of *Math1* mRNA expression in the developing ear (Fig. 6A), hindbrain region (Fig. 6A, inset), spinal cord, and other sites in the embryo (J.E.J., unpublished). By contrast, we were unable to detect GFP signal in the ears of *Math1*$^{-/-}$::Math1-GFP BAC embryos at stages E13.5 through E15.5 (Fig. 6B; data not shown), although GFP expression was clearly present at other sites of expression, such as the hindbrain (Fig. 6B, inset). A second transgenic line, which carries a 1.4 kb *Math1* enhancer with an E-box site that is essential for Math1 binding and autoregulation in other tissues (Helms et al., 2000), also mimics *Math1* expression in the developing wild-type ear (Chen et al., 2002; Lumpkin et al., 2003). As with the Math1-GFP BAC, we found no GFP reporter signal in the sensory epithelia of these *Math1*$^{-/-}$::Math1-GFP embryos at stages E13.5 through E15.5

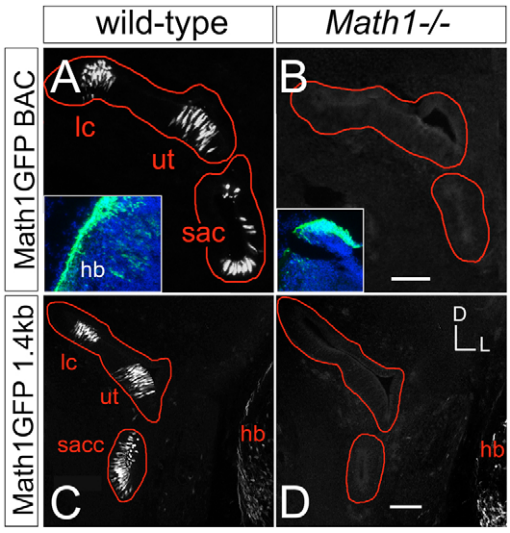

Fig. 6. Positive autoregulation of *Math1* in the otic epithelium. (**A**,**B**) Math1-GFP BAC transgene expression in wild-type and *Math1*$^{-/-}$ ears and hindbrain regions (insets). (**C**,**D**) 1.4 kb Math1-GFP transgene expression in wild-type and *Math1*$^{-/-}$ ears and hindbrain regions. lc, lateral crista; ut, utricle; sac, saccule; hb, hindbrain. Scale bars: 100 μm.

(Fig. 6C,D). The complete lack of reporter expression in the cristae of both *Math1*$^{-/-}$::Math1-GFP reporter lines indicates that the phenotype is not due solely to inhibition by ectopic expression of *Ngn1*.

DISCUSSION

The neurogenic region of the otocyst gives rise to sensory epithelia of the utricle and saccule

It has been unclear how neurogenic tissue of the otocyst relates to sensory epithelia of the inner ear. Gene expression studies in both chicken and mouse suggest that neurogenesis occupies only part of a larger sensory-competent domain of the otocyst (Morsli et al., 1998; Adam et al., 1998; Cole et al., 2000; Fekete and Wu, 2002), and a recent lineage study in the chicken shows that vestibular and spiral (auditory) neurons of the VIIIth ganglion can be clonally related to utricular epithelial cells (both macular and non-sensory) (Satoh and Fekete, 2005). By fate mapping in mouse, we show that *Ngn1*$^{+}$ otic epithelial cells can differentiate as vestibular or spiral ganglion neurons, hair or supporting cells of the utricular and saccular maculae, or non-sensory epithelial cells surrounding the maculae. Although the question remains open as to whether, in mouse, these cell types descend clonally from a common progenitor, our work unambiguously traces the origin of specific sensory (macular) and non-sensory cells to the neurogenic domain of the otocyst.

Our fate mapping suggests that the other functional class of vestibular sensory epithelia, the cristae, and their associated semicircular canals do not derive from the *Ngn1*$^{+}$ domain of the otocyst. This confirms previous gene expression studies tracing the origin of cristae to a *Bmp4*$^{+}$ region outside of, and adjacent to, the neurogenic domain (Morsli et al., 1998; Raft et al., 2004) (Fig. 7A′). The very rare occurrence (a few cells in one of 20 ears) of Ngn1 derivatives in the lateral crista suggests that mixing of cells between the neurogenic and *Bmp4* domains occurs infrequently. Whether this lack of mixing is due to differential affinity between the two regions, or whether neurogenesis is actively suppressed within the *Bmp4* domain, is not clear. In support of the latter hypothesis, *Tbx1*, a T-box gene that inhibits *Ngn1* and maintains *Bmp4* expression in the otocyst epithelium, is expressed continuously and from very early stages in the presumptive and definitive cristae (Arnold et al., 2006; Raft et al., 2004; Vitelli et al., 2003).

Our mapping of Ngn1-GFP and *NeuroD* expression domains revealed no evidence of active neurogenesis in the definitive cochlea. However, we did find Ngn1 derivatives in a non-sensory region of the cochlea (the GER) in the majority of ears analyzed. Based on its location in the ear, the GER might derive from the most posteroventral-medial edge of the otocyst neurogenic region. Interestingly, the GER lies immediately adjacent to the organ of Corti, within which we found no Ngn1 derivatives. This result, the common occurrence of Ngn1 derivatives in non-sensory tissue between the utricula macula and the anterior/lateral cristae (but not in the cristae) (Fig. 2E,G), and the initiation of macular *Math1* expression as stripes just within opposite borders of the neurogenic domain, support the hypothesis that sensory epithelia are induced at or near compartment boundaries in the otocyst (Fekete, 1996; Brigande et al., 2000).

Cross-inhibition between *Math1* and *Ngn1* segregates a progenitor field of dual competence into distinct neurogenic and sensory cell populations

We show that neurogenesis and hair cell production, long considered strictly sequential, actually overlap in the developing utricle and saccule for several days of gestation. During this period, neural precursors and nascent hair cells initially intermingle and later sort out across well-defined borders. Functionally, we show that *Math1* and *Ngn1* mutants have complementary inner ear phenotypes, supporting the hypothesis that mutual antagonism between these genes coordinates neurogenesis and hair cell production (Matei et al., 2005). Loss of *Math1*, which is normally expressed in all sensory regions of the ear, leads to excess and ectopic neurogenesis only in sensory regions with a history of *Ngn1* expression (utricular and saccular maculae). This effect is gene dose-sensitive, as *Math1* heterozygotes exhibit a neurogenic phenotype intermediate to those of the *Math1*-null homozygote and wild type. Conversely, *Ngn1* hemizygosity causes excess and ectopic *Math1* expression specifically in the utricle and saccule, and although *Ngn1*-null homozygosity causes growth abnormalities of the ear, the *Ngn1*$^{-/-}$ utricle still shows a phenotype of excess and ectopic *Math1* expression. These effects are seen only at sites in the developing ear where *Ngn1* and *Math1* are co-expressed, and we propose that they result from a disruption of close-range cross-inhibition. Cross-inhibition might influence multiple steps in the process, whereby an *Ngn1*$^{+}$ progenitor field of dual competence (neural and sensory epithelial) is gradually restricted to producing only sensory epithelial cells. These include: (1) *Math1* domain establishment within opposite borders of the *Ngn1*$^{+}$ region (Fig. 7A′); (2) *Math1* domain expansion and decline in *Ngn1* expression (Fig. 7A′,A″); and (3) compartmentalization of the region into a pair of adjacent *Math1* (sensory) and *Ngn1* (neurogenic) domains (Fig. 7A″). The potential basis for the competitive advantage of *Math1* over *Ngn1* in this system is discussed below.

Ngn1, but not *Math1*, functions as a proneural gene during mouse ear development

Criteria for proneural function include early, broad expression of transcript in all cells of a germinal epithelium and subsequent refinement of transcription to a subset of cells by lateral inhibition (Jan and Jan, 1993; Lewis, 1996). We find no evidence of these

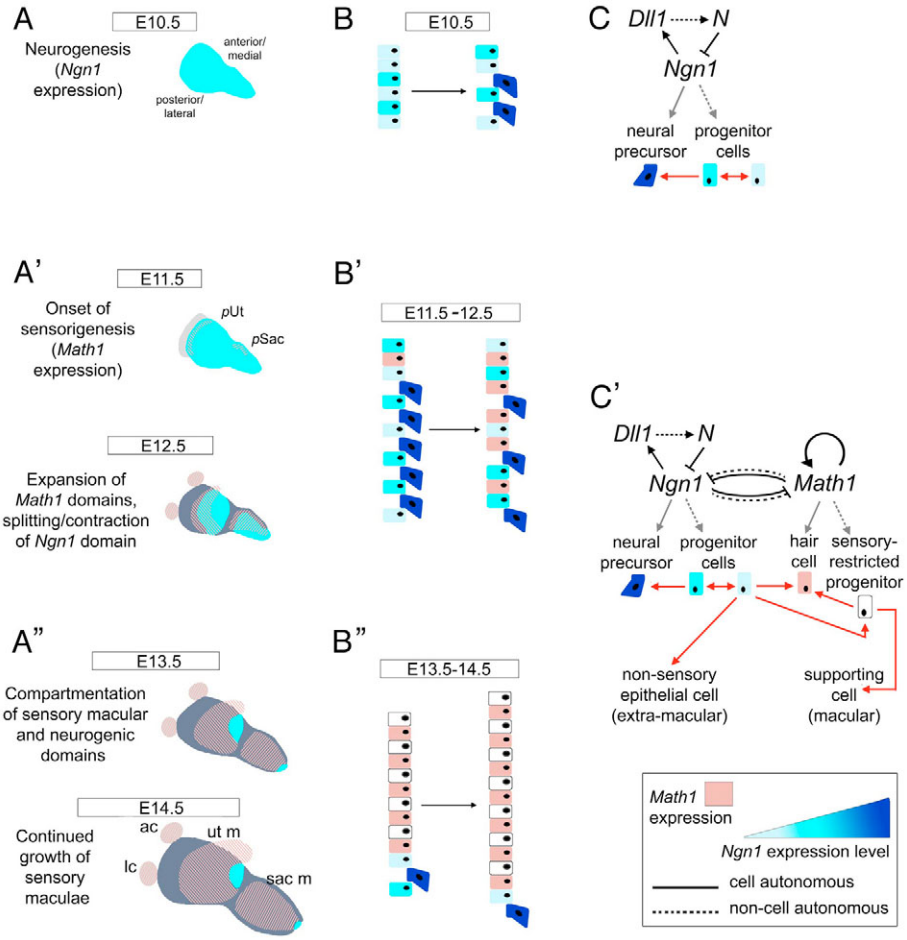

Fig. 7. A model of the transition from neurogenesis to sensory hair cell formation. (**A-A″**) Tissue-level changes in *Ngn1* expression (cyan), *Math1* expression (beige hatching), and regions where *Ngn1* expression has been extinguished (dark blue/gray) from E10.5-14.5. Light gray stripe at E11.5 represents *Bmp4* expression, which marks the prospective anterior and lateral cristae. *p*Ut, presumptive utricular macula; *p*Sac, presumptive saccular macula; ut m, utricular macula; sac m, saccular macula; ac, anterior crista; lc, lateral crista. (**B-B″**) Changes in gene expression and behavior (delamination) on a cellular scale and over short periods (denoted by arrows) in the neurogenic region of the otocyst (B), presumptive maculae (B′) and definitive maculae (B″). Shades of blue represent various intensities of *Ngn1* expression (see key). Beige represents *Math1*$^{+}$ cells. White represents cells expressing neither bHLH gene (sensory-restricted progenitors) that can differentiate as either hair or supporting cells. (**C**,**C′**) Genetic interactions (black lines), gene functions (gray lines) and cell fate transformations (red lines) before (C) and after (C′) the onset of *Math1* expression. *Dll1*, delta-like 1; *N*, Notch receptor. Solid gray and black lines indicate cell-autonomous interactions or functions. Dotted gray and black lines indicate non-cell-autonomous interactions or functions. Solid and dotted lines between *Ngn1* and *Math1* indicate that either, or both, mechanisms might mediate cross-inhibition.

features in our studies of *Math1* expression in the vestibular system of the mouse. Of the two genes relevant to this study, it is *Ngn1* and not *Math1* that initially marks the prospective maculae and exhibits the variegated expression among neighboring cells that is characteristic of proneural genes (Fig. 5A,B). Furthermore, using two different transgenic reporter lines, we show that *Math1* is required for detectable levels of *Math1* reporter expression in the otic epithelium, suggesting that *Math1* promoter activity is amplified and maintained by positive autoregulation. One possible consequence of this is a rapid and irreversible commitment of progenitors to the hair-cell fate once *Math1* transcription surpasses a threshold for positive autoregulation. Our results thus support the view that *Math1* functions as a hair-cell commitment factor rather than a proneural (or 'prosensory') gene (Chen et al., 2002) (for a review, see Kelley, 2006). Interestingly, in zebrafish, which has two *atoh1* genes, differences in the timing and autoregulation of *Math1*/*atoh1* genes from that described here lead to the opposite conclusion (Millimaki et al., 2007). For example, zebrafish *atoh1a* and *1b* are required for hair cell generation, but their expression precedes that of *ngn1* (Andermann et al., 2002) and marks the prospective maculae from very early stages. Gene duplication and evolutionary pressure on the regulatory genome might therefore dictate the precise functions of *Math1*/*atoh1* during ear development in different species.

Our experiments reveal a profile of *Ngn1* autoregulation very different from that of *Math1*. We demonstrate that *Ngn1* is required to limit its own transcription within the otic epithelium. We also extend a previous observation that proper otic expression of the Notch ligand *Dll1* is dependent on *Ngn1* (Ma et al., 1998) and show a pattern of increased *Ngn1* expression in the early otic epithelium of *Pofut1*$^{-/-}$ embryos, which are deficient in canonical Notch signaling (Shi and Stanley, 2003). These results and the expression of *Ngn1* in neural and sensory progenitors from very early stages fulfill several criteria for proneural function. Likely consequences of the proneural activity of *Ngn1* are control over the pace of neurogenesis during otocyst stages and preservation of an uncommitted progenitor cell population for sensory development. These functions are consistent with recently reported effects of conditional *Dll1* loss-of-function in the developing ear, which include an enlarged ganglion rudiment and specific hypoplasia of the utricle and saccule (Brooker et al., 2006), and with blockade of Notch signaling in the chicken, which causes excess neurogenesis at the expense of sensory epithelial precursors (Daudet et al., 2007).

Differences in bHLH gene autoregulation and cell behavior may direct the transition towards sensory epithelial formation

Given our evidence for a mutual antagonism between *Ngn1* and *Math1*, how does *Math1* exert the stronger inhibitory activity so that sensory epithelia replace an active neurogenic region? Our model states that *Ngn1* promotes a neural fate cell-autonomously and keeps its own expression low or off in neighboring cells through Notch-mediated lateral inhibition (Fig. 7B,C). Cells expressing high levels of *Ngn1* delaminate from the epithelium as neural precursors. Cells remaining within the neurogenic epithelium constitute a dynamic mix of committed neural precursors and uncommitted progenitors. The

latter group may adopt a neural fate in subsequent rounds of delamination or may remain uncommitted for several days, after which they adopt hair or supporting cell fates in response to *Math1* induction within the region (Fig. 7B′,B″,C′). This is supported by our fate mapping results, as Ngn1 derivatives can have any of these identities. Once *Math1* transcription exceeds a particular threshold, positive autoregulation irreversibly commits progenitors to a hair cell fate, and committed hair cells may then induce the supporting cell phenotype through intercellular signaling (Woods et al., 2004). Since strongly *Ngn1*$^+$ cells continuously delaminate from the epithelium, *Math1*-expressing cells are left to interact with epithelial progenitors expressing lower levels of *Ngn1*. These features might bias the mutual antagonism between *Ngn1* and *Math1*, thereby promoting sensory epithelial differentiation at the expense of continued neurogenesis.

Conclusion

We have implicated cross-regulation between bHLH genes and differential autoregulation as mechanisms for converting a neurogenic epithelium into specialized mechanosensory receptors. A novel aspect of this work – and one that is potentially relevant to other systems – is the dynamic nature of the patterning processes described. We show that progressive regionalization of bHLH genes through cross-inhibition can result in a sequential and overlapping production of distinct cell types, and that differential autoregulation might provide the driving force for such a transition.

Many questions remain unanswered. For example, does cross-inhibition between *Ngn1* and *Math1* occur within a single cell, through intercellular signaling, or by a combination of these two mechanisms? Cell-autonomous cross-inhibition might convert a weakly *Ngn1*$^+$ cell directly into a *Math1*$^+$ nascent hair cell. Alternatively, if the antagonism occurs through intercellular signaling, *Ngn1*$^+$ cells might pass through a ‘sensory-restricted progenitor’ state before committing to the hair-cell fate (Fig. 7C′). We find the latter alternative attractive given that embryonic maculae contain many Ngn1 derivatives with a pseudostratified epithelial (non-hair-cell) phenotype. Molecular and cellular mechanisms underlying the apparent compartmentalization of sensory and neurogenic regions also warrant scrutiny, as there is abundant evidence that Notch-mediated intercellular signaling occurs at nascent boundaries during development (Irvine, 1999). In summary, our results form a basis for understanding how progenitors are allocated to various cell fates during inner ear development.

We thank Huda Zoghbi and Pamela Stanley for providing *Math1* and *Pofut1* mutant mice; Jackie Lee, Qiufu Ma and Johannes Becker for in situ probes; and Juan Llamas, Welly Makmura and Sheri Juntilla for excellent colony maintenance. This work was supported by grants from the Mathers Charitable Foundation, the Alfred P. Sloan Foundation and the Medical Foundation (L.V.G.), and by NIH grants F32 DC007247 (S.R.), F31 DC007775 (E.J.K.), HD037932 and NS048887 (J.E.J.) and DC006185 (A.K.G. and N.S.).

Supplementary material

Supplementary material for this article is available at http://dev.biologists.org/cgi/content/full/134/24/4405/DC1

References

Adam, J., Myat, A., Le Roux, I., Eddison, M., Henrique, D., Ish-Horowicz, D. and Lewis, J. (1998). Cell fate choices and the expression of Notch, Delta, and Serrate homologues in the chick inner ear: parallels with Drosophila sense-organ development. *Development* **125**, 4645-4654.

Akagi, T., Inoue, T., Myoshi, G., Bessho, Y., Takahashi, M., Lee, J. E., Guillemot, F. and Kageyama, R. (2004). Requirement of multiple basic Helix-loop-helix genes for retinal neuronal subtype specification. *J. Biol. Chem.* **279**, 28492-28498.

Andermann, P., Ungos, J. and Raible, D. W. (2002). Neurogenin1 defines zebrafish cranial sensory ganglia precursors. *Dev. Biol.* **251**, 45-58.

Arnold, J. S., Braunstein, E. M., Ohyama, T., Groves, A. K., Adams, J. C., Brown, M. C. and Morrow, B. E. (2006). Tissue-specific roles of Tbx1 in the development of the outer, middle and inner ear, defective in 22q11DS patients. *Hum. Mol. Genet.* **15**, 1629-1639.

Barald, K. F. and Kelley, M. W. (2004). From placode to polarization: new tunes in inner ear development. *Development* **131**, 4119-4130.

Beckers, J., Clark, A., Wunsch, K., Hrabe De Angelis, M. and Gossler, A. (1999). Expression of the mouse Delta1 gene during organogenesis and fetal development. *Mech. Dev.* **84**, 165-168.

Ben-Arie, N., Bellen, H. J., Armstrong, D. L., McCall, A. E., Gordadze, P. R., Guo, Q., Matzuk, M. M. and Zoghbi, H. Y. (1997). Math1 is essential for genesis of cerebellar granule neurons. *Nature* **390**, 167-172.

Bermingham, N. A., Hassan, B. A., Price, S. D., Vollrath, M. A., Nissim, B.-A., Eatock, R. A., Bellen, H. J., Lysakowski, A. and Zoghbi, H. Y. (1999). Math1: An essential gene for the generation of inner ear hair cells. *Science* **284**, 1837-1841.

Bertrand, N., Castro, D. S. and Guillemot, F. (2002). Proneural genes and the specification of neural cell types. *Nat. Rev. Neurosci.* **3**, 517-530.

Brigande, J. V., Kiernan, A. E., Gao, X., Iten, L. E. and Fekete, D. M. (2000). Molecular genetics of pattern formation in the inner ear: Do compartment boundaries play a role? *Proc. Natl. Acad. Sci. USA* **97**, 11700-11706.

Brooker, R., Hozumi, K. and Lewis, J. (2006). Notch ligands with contrasting functions: Jagged1 and Delta1 in the mouse inner ear. *Development* **133**, 1277-1286.

Chen, P., Johnson, J. E., Zoghbi, H. Y. and Segil, N. (2002). The role of Math1 in inner ear development: uncoupling the establishment of the sensory primordium from hair cell fate determination. *Development* **129**, 2495-2505.

Cole, L. K., Le Roux, I., Nunes, F., Laufer, E., Lewis, J. and Wu, D. K. (2000). Sensory organ generation in the chicken inner ear: contributions of Bone Morphogenetic Protein 4, Serrate1, and Lunatic Fringe. *J. Comp. Neurol.* **424**, 509-520.

Cornell, R. A. and Eisen, J. S. (2002). Delta/Notch signaling promotes formation of zebrafish neural crest by repressing Neurogenin 1 function. *Development* **129**, 2639-2648.

D'Amico-Martel, A. and Noden, D. M. (1983). Contributions of placodal and neural crest cells to avian cranial peripheral ganglia. *Am. J. Anat.* **166**, 445-468.

Daudet, N., Ariza-McNaughton, L. and Lewis, J. (2007). Notch signaling is needed to maintain, but not to initiate, the formation of prosensory patches in the chick inner ear. *Development* **134**, 2369-2378.

Feil, R., Wagner, J., Metzger, D. and Chambon, P. (1997). Regulation of Cre recombinase activity by mutated estrogen receptor ligand-binding domains. *Biochem. Biophys. Res. Commun.* **28**, 752-757.

Fekete, D. M. (1996). Cell fate specification in the inner ear. *Curr. Opin. Neurobiol.* **6**, 533-541.

Fekete, D. M. and Wu, D. K. (2002). Revisiting cell fate specification in the inner ear. *Curr. Opin. Neurobiol.* **12**, 35-42.

Fode, C., Ma, Z., Casarosa, S., Ang, S.-L., Anderson, D. J. and Guillemot, F. (2000). A role for neural determination genes in specifying the dorsoventral identity of telencephalic neurons. *Genes Dev.* **14**, 67-80.

Fritzsch, B., Beisel, K. W., Jones, K., Farinas, I., Maklad, A., Lee, J. and Reichardt, L. F. (2002). Development and evolution of inner ear sensory epithelia and their innervation. *J. Neurobiol.* **53**, 143-156.

Gowan, K., Helms, A. W., Hunsaker, T. L., Collisson, T., Ebert, P. J., Odom, R. and Johnson, J. E. (2001). Crossinhibitory activities of Ngn1 and Math1 allow specification of distinct dorsal interneurons. *Neuron* **31**, 219-232.

Helms, A. W. and Johnson, J. E. (1998). Progenitors of dorsal commissural interneurons are defined by MATH1 expression. *Development* **125**, 919-925.

Helms, A. W., Abney, A. L., Ben-Arie, N., Zoghbi, H. Y. and Johnson, J. E. (2000). Autoregulation and multiple enhancers control Math1 expression in the developing nervous system. *Development* **127**, 1185-1196.

Inoue, T., Hojo, M., Sessho, Y., Tano, Y., Lee, J. E. and Kageyama, R. (2002). Math3 and NeuroD regulate amacrine cell fate specification in the retina. *Development* **129**, 831-842.

Irvine, K. D. (1999). Fringe, Notch, and making developmental boundaries. *Curr. Opin. Genet. Dev.* **9**, 434-441.

Izumikawa, M., Minoda, R., Kawamoto, K., Abrashkin, K. A., Swederski, D. L., Dolan, D. F., Brough, D. E. and Raphael. Y. (2005). Auditory hair cell replacement and hearing improvement by Atoh1 gene therapy in deaf mammals. *Nat. Med.* **11**, 271-276.

Jan, Y. N. and Jan, L. Y. (1993). HLH proteins, fly neurogenesis, and vertebrate myogenesis. *Cell* **75**, 827-830.

Kelley, M. W. (2006). Regulation of cell fate in the sensory epithelia of the inner ear. *Nat. Rev. Neurosci.* **7**, 837-849.

Kiernan, A. E., Steel, K. P. and Fekete, D. M. (2002). Development of the mouse inner ear. In *Mouse Development: Patterning, morphogenesis, and Organogenesis* (ed. J. Rossant and P. L. Tam), pp. 539-566. New York: Academic Press.

Lee, J. E., Hollenberg, S. M., Snider, L., Turner, D. L., Lipnick, N. and Wientraub, J. (1995). Conversion of Xenopus ectoderm into neurons by NeuroD, a basic helix-loop-helix protein. *Science* **268**, 836-844.

Lei, L., Xu, A., Panin, V. M. and Irvine, K. D. (2003). An O-fucose site in the ligand binding domain inhibits Notch activation. *Development* **130**, 6411-6421.
Lewis, J. (1996). Neurogenic genes and vertebrate neurogenesis. *Curr. Opin. Neurobiol.* **6**, 3-10.
Lumpkin, E. A., Collisson, T., Parab, P., Omer-Abdalla, A., Haeberle, H., Chen, P., Doetzlhofer, A., White, P., Groves, A. K., Segil, N. et al. (2003). Math1-driven GFP expression in the developing nervous system of transgenic mice. *Gene Expr. Patterns* **3**, 389-395.
Ma, Q., Kintner, C. and Anderson, D. J. (1996). Identification of neurogenin, a vertebrate neuronal determination gene. *Cell* **87**, 43-52.
Ma, Q., Chen, Z., del Barco Barantes, I., de la Ponpa, J. L. and Anderson, D. J. (1998). neurogenin1 is essential for the determination of neuronal precursors for proximal cranial sensory ganglia. *Neuron* **20**, 469-482.
Ma, Q., Anderson, D. J. and Fritzsch, B. (2000). Neurogenin1 null mutant ears develop fewer, morphologically normal hair cells in smaller sensory epithelia devoid of innervation. *J. Assoc. Res. Otolaryngol.* **1**, 129-143.
Matei, V., Pauley, S., Kaing, S., Rowitch, D., Beisel, K. W., Morris, K., Feng, F., Jones, K., Lee, J. and Fritzsch, B. (2005). Smaller inner ear epithelia in Neurog 1 null mice are related to earlier hair cell cycle exit. *Dev. Dyn.* **234**, 633-650.
Millimaki, B. B., Sweet, E. M., Dhason, M. S. and Riley, B. B. (2007). Zebrafish atoh1 genes: classic proneural activity in the inner ear and regulation by Fgf and Notch. *Development* **134**, 295-305.
Morsli, H., Choo, D., Ryan, A., Johnson, R. and Wu, D. K. (1998). Development of the mouse inner ear and origin of its sensory organs. *J. Neurosci.* **18**, 3327-3335.
Novak, A., Guo, C., Yang, W., Nagy, A. and Lobe, C. G. (2000). Z/EG, a double reporter mouse line that expresses enhanced green fluorescent protein upon Cre-mediated excision. *Genesis* **28**, 147-155.
Okajima, T. A., Xu, A. and Irvine, K. D. (2003). Modulation of notch-ligand binding by protein O-fucosyltransferase. *J. Biol. Chem.* **278**, 42340-42345.
Okajima, T. A., Xu, A., Lei, L. and Irvine, K. D. (2005). Chaperone activity of protein O-fucosyltransferase 1 promotes Notch receptor folding. *Science* **307**, 1599-1603.
Raft, S., Nowotschin, S., Liao, J. and Morrow, B. (2004). Suppression of neural fate and control of inner ear morphogenesis by Tbx1. *Development* **131**, 1801-1812.
Satoh, T. and Fekete, D. M. (2005). Clonal analysis of the relationships between mechanosensory cells and the neurons that innervate them in the chicken ear. *Development* **132**, 1687-1697.
Shailam, R., Lanford, P. J., Dolinsky, C. M., Norton, C. R., Gridley, T. and Kelley, M. W. (1999). Expression of proneural and neurogenic genes in the embryonic mammalian vestibular system. *J. Neurocytol.* **28**, 809-819.
Sher, A. E. (1971). The embryonic and postnatal development of the inner ear of the mouse. *Acta Otolaryngol. Suppl.* **285**, 5-77.
Shi, S. and Stanley, P. (2003). Protein O-fucosyltransferase 1 is an essential component of Notch signaling pathways. *Proc. Natl. Acad. Sci. USA* **100**, 5234-5239.
Stern, C. D. (1998). Detection of multiple gene products simultaneously by in situ hybridization and immunohistochemistry in whole mounts of avian embryos. *Curr. Top. Dev. Biol.* **36**, 223-243.
Vitelli, F., Viola, A., Morishima, M., Pramparo, T., Baldini, A. and Linsay, E. A. (2003). TBX1 is required for inner ear morphogenesis. *Hum. Mol. Genet.* **12**, 2041-2048.
Woods, C., Montcouquiol, M. and Kelley, M. W. (2004). Math1 regulates development of the sensory epithelium in the mammalian cochlea. *Nat. Neurosci.* **7**, 1310-1318.
Yang, X. W., Model, P. and Heintz, N. (1997). Homologous recombination based modification in Escherichia coli and germline transmission in transgenic mice of a bacterial artificial chromosome. *Nat. Biotechnol.* **15**, 859-865.
Zheng, J. L. and Gao, W. Q. (2000). Overexpression of Math1 induces robust production of extra hair cells in postnatal rat inner ears. *Nat. Neurosci.* **3**, 580-586.